Polymer Chemistry

# Synthesis and Photophysical Properties for Water-soluble Fluorinated Poly(aryleneethynylene)s

| | |
|---|---|
| Journal: | *Polymer Chemistry* |
| Manuscript ID | PY-ART-10-2018-001461.R1 |
| Article Type: | Paper |
| Date Submitted by the Author: | 25-Nov-2018 |
| Complete List of Authors: | Nose, Keiji; Doshisha University, Harris Science Research Institute<br>Noji, Katsuya; Tokyo Institute of Technology Interdisciplinary Graduate School of Science and Engineering<br>Iyoda, Tomokazu; Doshisha University, Harris Science Research Institute<br>Sanji, Takanobu; Tokyo Institute of Technology, Frontier Research Center |
| | |

Journal Name

ARTICLE

# Synthesis and Photophysical Properties for Water-soluble Fluorinated Poly(aryleneethynylene)s

う 5Received 00th January 20xx,
Accepted 00th January 20xx

DOI: 10.1039/x0xx00000x

**www.rsc.org/**

K. Nose,[a,b,c†] K. Noji,[a] T. Iyoda,[a,b,c†] T. Sanji[b]

**Herein, we report the synthesis of a new type of poly(aryleneethynylene)s (PAEs) comprising electron-deficient tetrafluoroarene units in the $\pi$-conjugated backbone and water-solubilizing oligoether (OE) side chains. The fluorinated PAEs were synthesized using a transition-metal-free polymerization system promoted by fluoride anions. Long OE side chains typically retard the polymerization. However, this is resolved by using a *t*BuOK initiator with a large excess of cryptand222. The present fluorinated PAEs display spectrophotometrically sufficient solubility in water, high fluorescence quantum yields, and reductive fluorescence quenching by arylamines.**

## Introduction

Water-soluble poly(aryleneethynylene)s (PAEs) have been widely investigated for sensing applications to detect metal ions, amino acids, proteins, live cells, and hazardous substances.[1-11] Sensing with conjugated polymers (CPs) has advantages over small molecules because of ease of development to the device using polymer wet-process,[12-14] scalable multivalent interaction to large biological analytes,[15] and exciton migration assisted enhancement of fluorescence quenching.[2] Various side chains have been designed to dissolve and functionalize CPs in water. Ionic side chains are powerful solubilization tools and are sensitive to ionic molecules, metal ions, and pH. Oligoether (OE) side chains are effective non-ionic units that make CPs water-soluble.[16-18] Non-ionic polymers are adequate for analysis of non-ionic weak interaction such as hydrogen bonds, the hydrophobic effect, electrostatics, and van der Waals forces. Weak interaction plays a central role in a biological system including protein folding, immune recognition, and DNA replication.

It has also been suggested that engineering polymer backbone of PAEs increases the chemosensory response. The majority of water-soluble CPs are electron-rich p-type,[19-22] and the number of electron-deficient n-type CPs remains limited. Nevertheless, several pyridinium-containing PAEs[3] and fluoroalkyl-substituted PAEs[14, 23] have been synthesized as n-type CPs for sensing applications, and these have proven to be effective chemosensors for electron-rich analytes. Arylamines are strong electron-rich molecules and especially important sensing target as hazardous substances,[24] amino acid metabolites, and biomarker for various diseases.[25] Main chain of non-ionic CPs should be engineered for sensing of these analytes in the biological system.

Fluorination of the polymer backbone is an effective strategy for lowering HOMO and LUMO energy levels, allowing the preparation of n-type CPs. Accordingly, fluorinated CPs have recently emerged as excellent candidates for organic semiconductors, widening the scope of available building blocks for organic electronics devices. Indeed, several top-performing semiconducting polymers have been developed by exploiting backbone fluorination.[26-34] In addition, fluorine can often exhibit non-covalent interactions, such as arene-perfluoroarene, fluorine-hydrogen, and fluorine-$\pi$ interactions,[35] in the formation of supramolecular complexes[36-40] or exciplexes[41, 42] with donor-conjugated molecules. These studies prompted us to develop water-soluble fluorinated CPs that interact with arylamines.

In the present study, we designed and synthesized water-soluble fluorinated PAEs having tetrafluoroarenes as the interactive units and OE side chains as water-solubilizing groups. We have reported the polymerization for fluorinated CPs under transition-metal-free condition.[43-45] Based on the study, we applied the system to the monomers in this work and investigated the synthetic system using *t*BuOK and cryptand222 (crypt-222) as the initiator of polymerization for long OE grafted PAEs. In addition, we investigated their photophysical properties and their interactions with

---

[a] *Interdisciplinary Graduate School of Science and Engineering, Innovative and Engineering Materials, Tokyo Institute of Technology, 4259 Nagatsuta, Midori-ku, Yokohama 226-8503, Japan.*
[b] *JST-ERATO Iyoda Supra-Integrated Material Project, Tokyo Institute of Technology, 4259-S2-3 Nagatsuta, Midori-ku, Yokohama 226-8503, Japan.*
[c] *Harris Science Research Institute, Doshisha University, 1-3 Miyakodani, Tatara, Kyotanabe City, 610-0394, Japan*
† Corresponding Author:
Email:tiyoda@mail.doshisha.ac.jp, knose@mail.doshisha.ac.jp

Electronic Supplementary Information (ESI) available: [Details on experimental methods, general procedures of syntheses, fluorescence and UV-Vis spectra]. See DOI: 10.1039/x0xx00000x arylamines as strong donors through reductive fluorescence quenching.

## Experimental

### Chemicals

CuI, $PdCl_2(PPh_3)_2$, triethylamine, 2-cyclohexylphosphino-2',6'-dimethoxy-1,1'-biphenyl, isopropylacetate, and $Pd(OAc)_2$ were purchased from Wako Pure Chemical Industries, Ltd. DMF and THF were used as a degassed anhydrous grade from Wako Pure Chemical Industries, Ltd. Triethylamine was distilled over $CaH_2$ and degassed. Silica gel for column chromatography was purchased from Wako Pure Chemical Industries, Ltd (Wakosil C-300, 40-64 μm or Wakosil HC-N, 35-63 μm). Aluminum oxide was purchased from Merck (Aluminum oxide 90 active neutral 63-200 μm). 2,5-Dibromohydroquinone and triisopropylsilylacetylene were purchased from Tokyo Chemical Industry Co., Ltd. Pentafluorobenzene, potassium t-butoxide (sublimed grade, 99.99% trace metals basis), tetrabutylammonium fluoride (TBAF, 1.0 M in THF), *N,N,N′,N′*-tetramethyl-p-phenylenediamine (TMPD) and aniline (AN) was purchased from Aldrich. The fluorometric grade solvents were used for measurement of UV-Vis spectra and fluorescence spectra. Water was purified on a Millipore Milli-Q water purification system. 2,6-Dimethylaniline (DMA) and *o*-toluidine (TL) was purchased from TCI and sublimed before use.

### Measurements

$^1$H, $^{13}$C, and $^{19}$F NMR spectra were recorded using a Bruker Biospin AVANCE 400 or 500 FT-NMR spectrometer at 400, 100, and 376(500, 125, and 471) MHz respectively. $^1$H and $^{13}$C chemical shifts were referenced to solvent residues. Mass and FAB mass spectra were obtained with a JEOL JMS-700 mass spectrometer. SEC (Size-Exclusion Chromatography) was performed at 40 °C on a JASCO HPLC LC-2000 Plus with RI detection and SHODEX LF804 (× 2) columns in THF as an eluent (1 mL·min−1). Molecular weights ($M_w$s) and molecular weight distributions were estimated on the basis of the polystyrene calibration standards. MALDI-TOF-MS was performed on a Shimadzu/Kratos AXIMA-CFR plus with an acceleration voltage of 20 kV, a delay time of 100 ns, in the reflector mode. The samples for MALDI-TOF-MS analysis were dissolved in THF a concentration of 1mg mL-1. Dithranol (1,8-dihydroxy-9[10H]-anthracenone) was used as the matrix and was dissolved in THF to a concentration of 10 mg mL-1. Sodium trifluoroacetate (TFANa) was used as a cationization reagent was dissolved in THF to a concentration of 10 mg mL$^{-1}$. The solution of the matrix, the polymer, and TFANa were mixed in a 1:1:1 volume ratio. Other materials were purchased from commercial sources and used without further purification unless otherwise noted. UV-Vis spectra were recorded with a Shimadzu SolidSpec-3700. Fluorescence spectra were obtained with a Jasco FP-6300 spectrofluorometer. Quantum efficiencies were measured with a Quantaurus-QY Absolute PL quantum yield spectrometer (Hamamatsu Photonics K. K.). Fluorescent life times were recorded using a Quantaurus-Tau Fluorescence lifetime spectrometer (Hamamatsu Photonics K. K.).

### Polymerization of 1

In a reaction flask under Ar, **1**(187.2 mg, 0.25 mmol) and THF (5 mL) were added. TBAF (0.1 M THF solution, 50 μL, 5× 10$^{-3}$ mmol, 2 mol%) was then added, and the solution was stirred at room temperature for 30 min. After stirring, the mixture was poured into ether (100 mL). The precipitate was collected by centrifugation. A second cycle of dissolving–precipitation followed by freeze-drying gave the polymer (66 mg, 0.189 mmol for the polymer repeating unit, 75%) as a pale yellow solid. A pale yellow solid: $M_n$ = 11200, PDI = 1.6 (SEC relative to polystyrene standards); $^1$H NMR (400 MHz, $CD_2Cl_2$) δ 3.31-4.24 (bm), 6.97(bm), 7.31(bm); $^{19}$F NMR (376 MHz, CD2Cl2) δ −163.82-−163.91 (bm), −156.22-−156.17 (bm), −141.08-−140.37 (bm), −138.40-−138.37 (bm).

### Polymerization of 2

In a reaction flask under Ar, **2** (160.4 mg, 0.1 mmol), cryptand[2.2.2] (181.4 mg, 0.5 mmol), and THF (2 mL) were added. Potassium t-butoxide (0.1 M THF solution, 20 μL, 2× 10-3 mmol, 4 mol%) was then added, and the solution was stirred at 50 ºC for 42 hours. After stirring the mixture was poured into hexane (100 mL). The precipitate was collected by centrifugation and purified with preparative GPC (chloroform). After removal solvent, a second cycle of dissolving–precipitation followed by freeze-drying gave the polymer (96 mg, 0.067 mmol for the polymer repeating unit, 67%) as a pale yellow greasy oil. A pale yellow greasy oil: $M_n$ = 20900, PDI = 2.1 (SEC relative to polystyrene standards); $^1$H NMR (400 MHz, $CD_2Cl_2$) δ 3.33-4.24 (bm), 6.94-6.97(bm), 7.26-7.31(bm); $^{19}$F NMR (376MHz, $CD_2Cl_2$) δ −163.86-−163.72 (bm), −156.08 (bm), −141.15-−140.17 (bm), −138.53-−138.02 (bm).

### Polymerization of 3

In a reaction flask under Ar, **3** (121.8 mg, 0.1 mmol), cryptand[2.2.2] (181.4 mg, 0.5 mmol), and THF (2 mL) were added. Potassium t-butoxide (0.1 M THF solution, 30 μL, 3× 10-3 mmol, 3 mol%) was then added, and the solution was stirred at 50 ºC for 24 hours. After stirring the mixture was poured into hexane (100 mL). The precipitate was collected by centrifugation and purified with preparative GPC (chloroform). After removal solvent, a second cycle of dissolving–precipitation followed by freeze-drying gave the polymer (84mg, 0.08 mmol for the polymer repeating unit, 81%) as a pale yellow greasy oil. A pale yellow greasy oil: $M_n$ = 20660, PDI = 2.9 (SEC relative to polystyrene standards); $^1$H NMR (400 MHz, $CD_2Cl_2$) δ 2.28-2.45 (bm), 3.31-4.15 (bm), 6.89-6.97(bm), 7.27-7.30(bm); $^{19}$F NMR (376 MHz , $CD_2Cl_2$) δ −163.86-−163.77 (bm), −156.03—155.97 (bm), −141.00-−140.18 (bm), −138.53-−138.36 (bm).

### Fluorescence quenching experiment

The experiments were performed under an inert argon atmosphere. The polymer solution added to the cell. A syringe filled with quencher solution was inserted through the septum on the cell. These procedures up to this point was done inside the glovebox. After that, the cell was moved to the spectrometer located outside the glovebox. TMPD was sublimed under vacuum before use. AN, DMA, and TL were distilled over NaOH under Ar. Solvent was degassed by freeze-pump-thaw cycles. All quenchers were stored in the glove box.

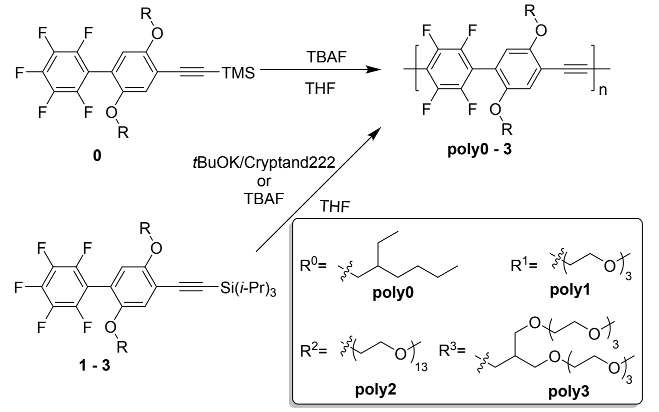

**Scheme 1** Synthesis of fluorinated PAEs with a catalytic amount of TBAF or *t*BuOK/crypt-222.

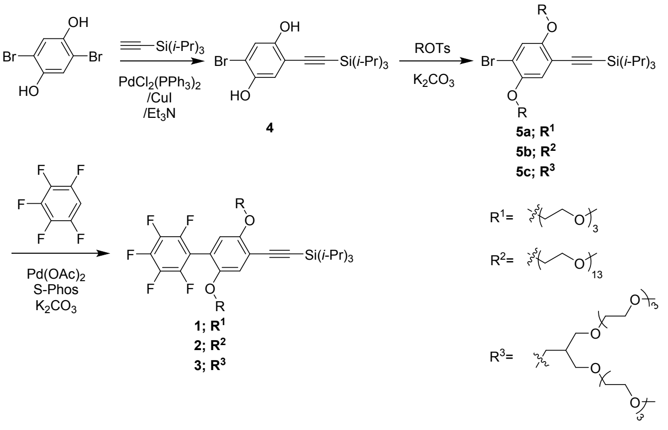

**Scheme 2** Synthesis of **1-3**.

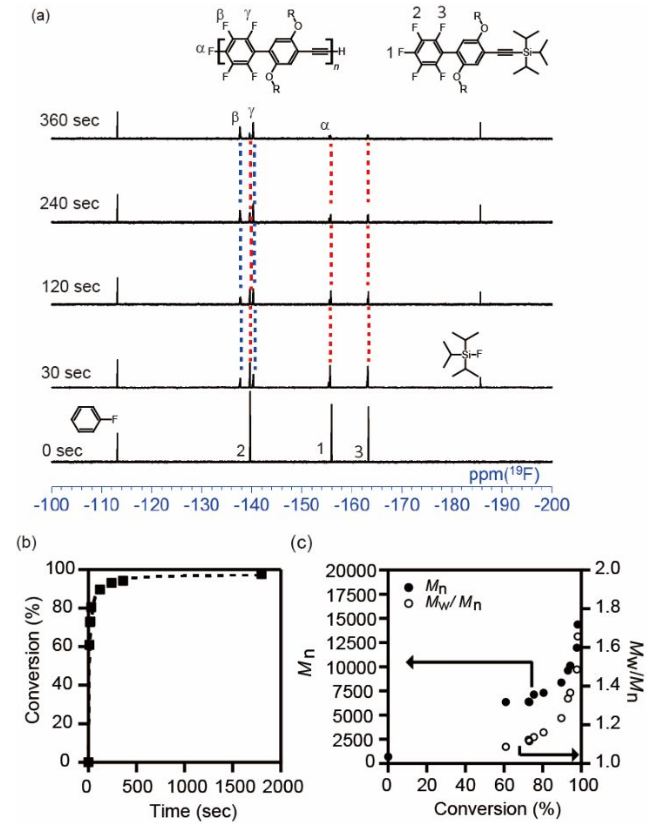

**Fig. 1** (a) $^{19}$F NMR spectra for the polymerization of **1**(50mM) with 2 mol% TBAF in THF at room temperature (CDCl$_3$). Fluorobenzene was used as the internal standard. (b) Conversion of **1** as a function of time calculated from $^{19}$F NMR spectra. (c) $M_w/M_n$ (blank circle) and $M_n$ (circle) as a function of conversion of **1**.

## Results and Discussion

### Monomer synthesis

We designed AB-type monomers having oligoether (OE) side chains as water-solubilizing groups. A new synthetic strategy was developed for accessing OE grafted monomers. The monomers **1-3** were obtained through three steps from commercially available 2,5-dibromohydroquinone as depicted in Scheme 2. Initially, **4** was prepared by the Sonogashira cross-coupling of 2,5-dibromohydroquinone with tris(isopropyl)silylacetylene. Then, OE side chains were introduced by the reaction of **4** and ROTs to give **5a**-**5c**. Reaction pentafluorobenzene and **5a-c** in the presence of palladium acetate and dicyclohexyl(2',6'-dimethoxybiphenyl-2-yl)phosphan (S-Phos) afforded the monomers **1-3**.

All compounds were characterized by the NMR and HRMS spectra (see the ESI†).

### Polymerization of 1

To render the polymers hydrophilic, we introduced OE side chains to the PAEs (Scheme 1). Polymerization of the fluorinated PAEs was employed based on a method previously reported by our group that proceeds under transition-metal-free conditions.[44]

The fluoride ion acts as both the initiator and the catalyst for the self-condensation between a pentafluorophenyl and a trimethylsilyl (TMS) group in monomer **0** through an S$_N$Ar reaction that occurs selectively at the 4-fluorine position. **Poly0** can be synthesized using the same procedure as that used for monomer **0** with 1 mol% tetrabutylammonium fluoride (TBAF) as the initiator in THF at room temperature.[44]

We applied the polymerization system to monomer **1**, in which the TMS group is replaced by tris(isopropyl)silyl (TIPS) group owing to synthetic difficulties with the former, using 2 mol% TBAF in THF at room temperature and successfully obtained **poly1** in 75% yield. The polymerization was monitored as a function of the reaction time using $^{19}$F NMR spectra of the reaction mixture after quenching with ethanol (Fig. 1a). The signals at -137.6 and -140.3 ppm were assigned to fluorine substituents, β and γ, of perfluoroarene moieties of the polymer, respectively, judging from time evolution of relative peak intensity. As the reaction time increases, the signals corresponding to the polymer and tris(isopropyl)silyl fluoride (TIPSF) at −185.7 ppm increase. TIPSF is the releasing molecule caused by the attack to TIPS with TBAF, supporting the reaction mechanism in previous report[45]. In Fig. 1b, monomer conversion was plotted again reaction time. The degree of polymerization at 1800 sec was estimated to be 12 calculated by dividing averaged integral values for β and γ by α. This polymerization proceeds quickly and completes within 5 min. The number average molecular weight ($M_n$) of the resulting **poly1** increases more rapidly than that expected for ideal step-growth polymerization at the initial stage of polymerization, and after that increases rapidly. The polydispersity ($M_w/M_n$) is less than 1.3 in the initial stage. However, $M_w/M_n$ increases rapidly above 80% monomer conversion (Fig. 1c). In the previous study[44], we reported that polymerization in this system proceeds in a chain-growth manner, although some chain-transfer occurs depending on monomer structure.

### Polymerization of 2 and 3

One issue regarding the syntheses of the PAEs is the lower reactivity of monomers **2** and **3**, which is probably due to the large OE side chains. The polymerizations of **2** and **3** do not proceed well using TBAF as the initiator (Table S1 and Fig. S11). Consequently, we modified the previously reported method,[44] incorporating *t*BuOK/crypt-222 as the initiator in an attempt to overcome the problem of lower reactivity. We found that *t*BuOK with a large excess of crypt-222 activates the polymerization, yielding high-molecular-weight polymers. The concentration of crypt-222 required is 250-times that of the reaction sites.

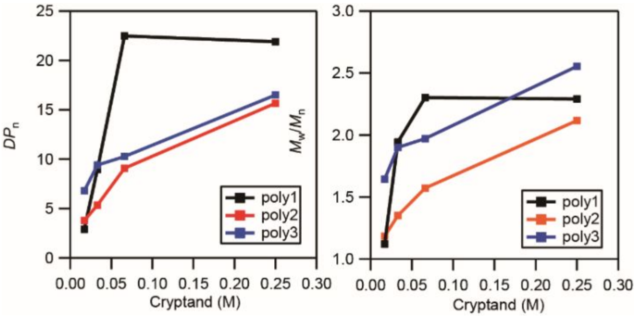

**Fig. 2.** The degree of polymerization ($DP_n$, left) and $M_w/M_n$ (right) of **poly1–3** as a function of the concentration of crypt-222. The polymerizations were performed with 2 mM *t*BuOK and 50 mM monomer in THF at 50 °C.

This polymerization system was used to obtain **poly2** and **poly3**, as described in the following section. The characterization of the polymers was conducted by $^1$H NMR, SEC, and MALDI-TOF-MS (see Figs. S8–S10). The MALDI-TOF-MS trace for **poly3** (Fig. S10) shows peaks that can be assigned to both the 4-*tert*-butyloxy-2,3,5,6-tetrafluoroarene groups and the terminal pentafluoroarene groups, indicating that *t*BuOK acts as an initiator that attacks both pentafluorophenyl and trimethylisopropyl groups. To obtain further insight into these phenomena, we conducted the polymerization of **poly1-3** with different concentrations of crypt-222. Fig. 2 shows the number-average degree of polymerization ($DP_n$) and $M_w/M_n$ for the obtained polymers as functions of the concentration of crypt-222 when the polymerizations were conducted using 4 mol% *t*BuOK. The $DP_n$ of **poly2** increases from 3 to 15 as the concentration of crypt-222 increases (Table S2). In addition, large side chains on the polymers result in smaller values of $DP_n$. One possible explanation for the differences in reactivity for monomers with different side chains is that the growing tip of the polymer is negatively charged and paired with a potassium cation, but larger OE side chains surround the potassium cation and prevent access of further monomers to the growing tip. Crypt-222 can capture the potassium cation from the ion pair and, as a result, its inherent reactivity is recovered (Fig. S12).

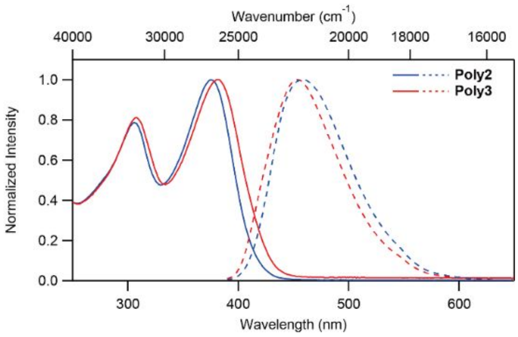

**Fig. 3** Absorption (solid line) and fluorescence spectra (dotted line) of **poly2–3** in water at room temperature.

**Table 1** Physical and photophysical properties of the PAEs prepared in this study

| Sample | $M_n$ (PDI)$^{a)}$ | Medium | Absorption $\lambda_{max}$ / nm | Fluorescence $\lambda_{max}$ / nm | Fluorescence quantum yield ($\phi$) / % $^{b)}$ | Fluorescence lifetime ($\tau$) / ns $^{b)}$ | Solubility / mM |
|---|---|---|---|---|---|---|---|
| **poly0** | $8.8 \times 10^3$ (2.0) | THF | 380 | 437 | 76.0 | 1.29 | >5 |
| | | Thin film | 369 | 438 | 42.9 | 0.74 | |
| **poly1** | $1.1 \times 10^4$ (1.6) | THF | 381 | 442 | 69.2 | 1.36 | >5 |
| | | Thin film | 374 | 462 | 40.7 | 1.17 | |
| **poly2** | $1.1 \times 10^4$ (1.6) | Water | 375 | 456 | 44.4 | 1.57 | 0.8 |
| | | THF | 374 | 449 | 56.7 | 1.55 | >5 |
| | | Thin film | 375 | 456 | 34.9 | 1.22 | |
| **poly3** | $8.2 \times 10^3$ (1.9) | Water | 382 | 454 | 43.2 | 1.82 | 0.1 |
| | | THF | 375 | 443 | 67.5 | 1.28 | >5 |
| | | Thin film | 384 | 456 | 44.9 | 1.46 | |

$^{a)}$ $M_n$ was obtained using SEC. $^{b)}$ Under Ar atmosphere.

### Photophysical properties

The OE side chains broaden the range of solvents that dissolve the polymers from halogenated and etheric ones to alcohols and water, for which the solubilities exceed spectroscopic use. (Table S3) For example, **poly2** exhibits water-solubility of 0.8 mM per repeat unit (PRU). Table 1 summarizes the photophysical properties of the PAEs in water, THF, and in thin films. The UV-Vis spectra of the PAEs present $\lambda_{max}$ at 375–381 nm in THF, which are shorter wavelengths than those of conventional PAEs[17] because of the large dihedral angles between the perfluorophenyl and OE-substituted phenyl rings in the main chain. **Poly2** and **poly3** show shorter $\lambda_{max}$ values in THF than **poly0** and **poly1** since sterically large side chains increase this dihedral angle.

The absorption spectra in THF and water do not differ significantly (Figs. 3 and S14). **Poly2** and **poly3** exhibit high fluorescence quantum yields (44.4 and 43.2%, respectively) in water at room temperature under Ar. This is because the large OE side chains prevent aggregation of the polymer and thus self-quenching. The absorption of **poly2** obeys the Lambert-Beer law from $1.0 \times 10^{-7}$ to $2.0 \times 10^{-4}$ M (Fig. S15). A fascinating feature of this system is that the spectroscopic properties are independent of the media. This feature makes these materials particularly suitable for solid-state applications in organic electronics. In general, PAEs display red-shifted absorption as solid films compared to that in solution owing to aggregation of the polymer backbone,[46] which often causes fluorescence self-quenching.

### Quenching experiment with arylamines

Arylamines are strong donors and form complexes with fluorinated arene compounds.[41, 42] To study the interactions between the polymers and such arylamines, we performed fluorescence quenching experiments with **poly2** ($2.3 \times 10^{-6}$ M PRU in water) with aniline (AN), 2-methylaniline (MA), 2,6-dimethylaniline (DMA), and *N,N,N′,N′*-tetramethyl-*p*-phenylenediamine (TMPD) as fluorescence quenchers. The fluorescence intensity of **poly2** decreases as the concentration of these amines increases (Figs. 4 and S16) but their $F_0/F$ vs. [Q] plots present upward curves (Fig. 4b), indicating both static and dynamic quenching.

Combined static and dynamic quenching is described by the following equation:

$$\frac{F_0}{F} = (1 + K_s[Q])(1 + k_q\tau_0[Q]) \qquad (1)$$

where $F_0$, F, [Q], $k_q$, and $\tau$ are the fluorescence intensities with and without quencher, the concentration of the quencher, the bimolecular quenching constant, and fluorescence lifetime, respectively. The value of the term in the second parenthesis can be determined from a lifetime-based Stern-Volmer plot, $\tau_0/\tau = 1+k_q\tau_0[Q]$. The value of $k_q$ determined from the slope (Fig. 4d) is $1.0\times 10^{10}$–$2.1 \times 10^{10}$ $M^{-1}$ $s^{-1}$ similar to the diffusion-controlled limit, implying a dynamic quenching process. The first parenthesis corresponds to static quenching, which occurs because of the formation of a ground-state complex with the quencher. $K_s$ is the association constant for this complex, which is the slope of Stern-Volmer plot under low concentration of quenchers (Fig. 4c). As the oxidation potential of the quencher becomes cathodic, *i.e.*, it becomes more easily oxidized, $K_s$ increases, as is typically observed for charge-transfer interactions. Indeed, $K_s$ is highest among the arylamines investigated for TMPD ($E_{ox}$= 0.27,[47] $K_s$ = 549 $M^{-1}$) because of the strong electron-donating dimethylamino group. The methyl group, which is a weak electron donor, leads to the higher $K_s$ values for MA ($E_{ox}$=0.60,[48] $K_s$ = 151 $M^{-1}$) and DMA ($E_{ox}$=0.57,[48] $K_s$ = 330 $M^{-1}$) than that of AN ($E_{ox}$=0.63,[48] $K_s$ = 89 $M^{-1}$). These values of the sensitivity for aryl amines are higher than those of previously reported material.[24]

As a control experiment, we demonstrated quenching using polyfluorene as a conventional p-type CP; however, AN does not quench its fluorescence in THF (Fig. S17). Quenching of **poly2** with AN in THF results in a lower $K_s$ than that in water (Fig. S18, indicating that a highly polar solvent allows for stabilization of the ground-state complex. A decrease in the absorption band at 375 nm for **poly2** is observed as the concentration of the quencher increases (Fig. S19), which constitutes additional evidence for the static quenching mechanism.

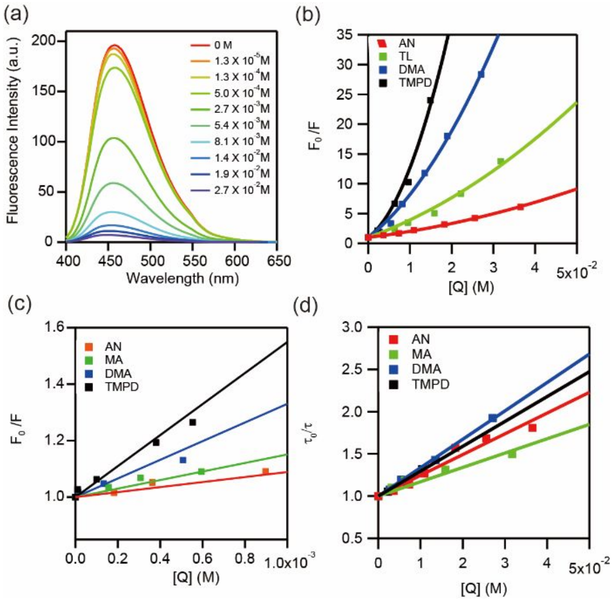

**Fig. 4** (a) Fluorescence spectra of **poly2** in water upon addition of DMA. The excitation wavelength was 380 nm. (b) Stern-Volmer plot for fluorescence quenching at $\lambda_{max}$, (c) expansion of the concentration for the same experimental data as in Figure 3b, and (d) lifetime Stern-Volmer plot for **poly2** in water in response to AN (red), MA (green), DMA (blue), and TMPD (black).

## Conclusions

In summary, we have developed water-soluble fluorinated n-type PAEs that work as fluorescence sensing materials on arylamines through non-ionic weak interaction. Trimeric OE substituted monomer **1** can be polymerized by previous reported method using TBAF. Long OE sidechains reduce the reactivity of the polymerization. *t*BuOK and a large excess of crypt-222 resolved the problem to yields the polymers. One of the obtained polymers, 13-meric OE PAE **poly2**, exhibits a high-fluorescence quantum yield and a fluorescence-quenching response to arylamines that proceeds by combined static and dynamic quenching. This work present a novel strategy for the possibility of the use of fluorinated PAEs as sensing materials for weak interaction. The present polymer would be good candidate for the building block of interactive $\pi$-conjugated molecular devices such as metal organic framework (MOF), covalent organic framework (COF), polymer brush, and single molecular circuit.

## Acknowledgment

This work was supported by JST ERATO Grant Number JPMJER1001 and JSPS KAKENHI Grant Number 16H02299.

## Conflicts of interest

There are no conflicts of interest to declare.

## Notes and references

1 U. H. F. Bunz, *Macromol. Rapid Commun.*, 2009, **30**, 772-805.
2 U. H. F. Bunz, K. Seehafer, M. Bender and M. Porz, *Chem. Soc. Rev.*, 2015, **44**, 4322-4336.
3 S. Rochat and T. M. Swager, *J. Am. Chem. Soc.*, 2013, **135**, 17703-17706.
4 M. D. Disney, J. Zheng, T. M. Swager and P. H. Seeberger, *J. Am. Chem. Soc.*, 2004, **126**, 13343-13346.
5 B. Liu and G. C. Bazan, *Chem. Mater.*, 2004, **16**, 4467-4476.
6 I. B. Kim, A. Dunkhorst and U. H. F. Bunz, *Langmuir*, 2005, **21**, 7985-7989.
7 I. B. Kim, J. N. Wilson and U. H. F. Bunz, *Chem. Commun.*, 2005, DOI: 10.1039/b416587j, 1273-1275.
8 J. H. Moon, W. McDaniel, P. Maclean and L. F. Hancock, *Angew. Chem. Int. Ed. Engl.*, 2007, **46**, 8223-8225.
9 R. L. Phillips, I. B. Kim, L. M. Tolbert and U. H. F. Bunz, *J. Am. Chem. Soc.*, 2008, **130**, 6952-6954.
10 R. L. Phillips, I.-B. Kim, B. E. Carson, B. Tidbeck, Y. Bai, T. L. Lowary, L. M. Tolbert and U. H. F. Bunz, *Macromolecules*, 2008, **41**, 7316-7320.
11 K. Seehafer, M. Bender, S. T. Schwaebel and U. H. F. Bunz, *Macromolecules*, 2014, **47**, 7014-7020.
12 J.-S. Yang and T. M. Swager, *J. Am. Chem. Soc.*, 1998, **120**, 11864-11873.
13 H. Kim, Y. Kim and J. Y. Chang, *Macromol. Chem. Phys.*, 2014, **215**, 1274-1285.
14 Y. Kim, J. E. Whitten and T. M. Swager, *J. Am. Chem. Soc.*, 2005, **127**, 12122-12130.
15 M. Mammen, S.-K. Choi and G. M. Whitesides, *Angew. Chem. Int. Ed.*, 1998, **37**, 2754-2794.
16 J. Mei and Z. Bao, *Chem. Mater.*, 2014, **26**, 604-615.
17 A. Khan, S. Muller and S. Hecht, *Chem. Commun.*, 2005, DOI: 10.1039/b413616k, 584-586.
18 K. Lee, H. J. Kim and J. Kim, *Adv. Funct. Mater.*, 2012, **22**, 1076-1086.
19 K. Y. Pu and B. Liu, *Biosensors & Bioelectronics*, 2009, **24**, 1067-1073.
20 K. Li and B. Liu, *Polymer Chemistry*, 2010, **1**, 252-259.
21 J. Liu, G. Feng, J. Geng and B. Liu, *ACS Applied Materials & Interfaces*, 2013, **5**, 4511-4515.
22 L. Zhou, J. Geng, G. Wang, J. Liu and B. Liu, *Polymer Chemistry*, 2013, **4**, 5243.
23 Y. Kim and T. M. Swager, *Macromolecules*, 2006, **39**, 5177-5179.
24 Y.-J. Zhao, K. Miao, Z. Zhu and L.-J. Fan, *ACS Sensors*, 2017, **2**, 842-847.
25 M. Gao, S. Li, Y. Lin, Y. Geng, X. Ling, L. Wang, A. Qin and B. Z. Tang, *ACS Sensors*, 2016, **1**, 179-184.
26 C.-C. Chen, W.-H. Chang, K. Yoshimura, K. Ohya, J. You, J. Gao, Z. Hong and Y. Yang, *Advanced Materials*, 2014, **26**, 5670-5677.
27 J.-D. Chen, C. Cui, Y.-Q. Li, L. Zhou, Q.-D. Ou, C. Li, Y. Li and J.-X. Tang, *Advanced Materials*, 2015, **27**, 1035-1041.
28 Y.-J. Hwang, B. A. E. Courtright, A. S. Ferreira, S. H. Tolbert and S. A. Jenekhe, *Advanced Materials*, 2015, **27**, 4578-4584.
29 N. Leclerc, P. Chavez, O. A. Ibraikulov, T. Heiser and P. Leveque, *Polymers*, 2016, **8**.
30 C. Liu, C. Yi, K. Wang, Y. Yang, R. S. Bhatta, M. Tsige, S. Xiao and X. Gong, *ACS Applied Materials & Interfaces*, 2015, **7**, 4928-4935.
31 Y. Liu, J. Zhao, Z. Li, C. Mu, W. Ma, H. Hu, K. Jiang, H. Lin, H. Ade and H. Yan, *Nature Communications*, 2014, **5**, 5293.
32 T. S. van der Poll, J. A. Love, T.-Q. Nguyen and G. C. Bazan, *Advanced Materials*, 2012, **24**, 3646-3649.
33 J. You, L. Dou, K. Yoshimura, T. Kato, K. Ohya, T. Moriarty, K. Emery, C.-C. Chen, J. Gao, G. Li and Y. Yang, *Nature Communications*, 2013, **4**, 1446.
34 A. Zhang, C. Xiao, Y. Wu, C. Li, Y. Ji, L. Li, W. Hu, Z. Wang, W. Ma and W. Li, *Macromolecules*, 2016, DOI: 10.1021/acs.macromol.6b01446.
35 Q. Zhang, M. A. Kelly, N. Bauer and W. You, *Accounts of Chemical Research*, 2017, **50**, 2401-2409.
36 C. R. Patrick and G. S. Prosser, *Nature*, 1960, **187**, 1021-1021.
37 G. W. Coates, A. R. Dunn, L. M. Henling, D. A. Dougherty and R. H. Grubbs, *Angewandte Chemie-International Edition in English*, 1997, **36**, 248-251.
38 A. F. M. Kilbinger and R. H. Grubbs, *Angewandte Chemie-International Edition*, 2002, **41**, 1563-1566.
39 S. S. Babu, V. K. Praveen, S. Prasanthkumar and A. Ajayaghosh, *Chem. Eur. J.*, 2008, **14**, 9577-9584.
40 X. H. Zhou, J. D. Luo, S. Huang, T. D. Kim, Z. W. Shi, Y. J. Cheng, S. H. Jang, D. B. Knorr, R. M. Overney and A. K. Y. Jen, *Adv. Mater.*, 2009, **21**, 1976-1981.
41 M. L. Renak, G. P. Bartholomew, S. J. Wang, P. J. Ricatto, R. J. Lachicotte and G. C. Bazan, *J. Am. Chem. Soc.*, 1999, **121**, 7787-7799.
42 S. J. Wang and G. C. Bazan, *Chem. Phys. Lett.*, 2001, **333**, 437-443.
43 T. Sanji and T. Iyoda, *J. Am. Chem. Soc.*, 2014, **136**, 10238-10241.
44 T. Sanji, A. Motoshige, H. Komiyama, J. Kakinuma, R. Ushikubo, S. Watanabe and T. Iyoda, *Chem Sci*, 2015, **6**, 492-496.
45 T. Sanji, K. Nose, J. Kakinuma and T. Iyoda, *Polymer Chemistry*, 2016, **7**, 7116-7125.
46 A. Kraft, A. C. Grimsdale and A. B. Holmes, *Angew Chem Int Edit*, 1998, **37**, 402-428.
47 S. Steenken and P. Neta, *The Journal of Physical Chemistry*, 1982, **86**, 3661-3667.

48 P. Winget, E. J. Weber, C. J. Cramer and D. G. Truhlar, *Phys. Chem. Chem. Phys.*, 2000, **2**, 1231-1239.

Reported are the synthesis of water-soluble fluorinated conjugated polymers, and photophysical properties, and fluorescent quenching response to arylamines.